# POD methods used in the analysis of the heat transport in the Solar Corona

Diana Gamborino Uzcanga, ICN-UNAM
Diego del Castillo Negrete, ORNL-EUA
y Julio J. Martinell, ICN-UNAM

# Abstract

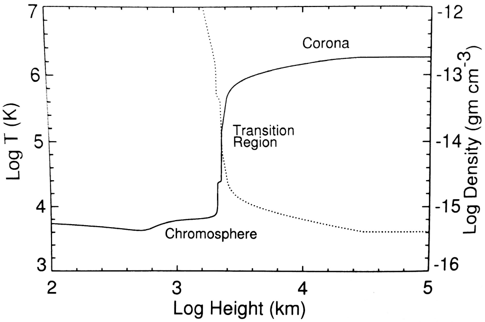


-Solar Corona heating mechanisms still not clear.

- Energy released mainly in AR - propagated to other regions - maintain Corona at observed T.

- Global heat transport influenced by complex $\vec{B}$ geometry that couples distant regions of Corona.

- Produce nonlocal effects in the transport.

- EUV images - AIA/SDO.Three cases: (a) following an explosive event, (b) five hours before the explosive event, same AR and (c) Quiet Sun region.

- SolarSoft - T Maps- full solar disk.

- Regions of interest - selected and analyzed with POD methods.

- (1) Topos-Chronos: Energy cascade process determined -subdiffusion.

- (2) GLRAM: $w \sim t^{\gamma}$. W found $\gamma < 1$ : subdiffusion.

# Temperature Maps

## SolarSoft

- AIA/SDO EUV filters: 94, 131, 171, 193, 211, 334 Å.
- Temperature resolution: 27 equi-spaced values in log scale $\log T = 5.7 - 7.0$ equivalent to $T = 0.5 - 10$ MK.
- Maps have 1/10 th of original maps spatial resolution.
- Conversion to ASCII format to analyze with MatLab.

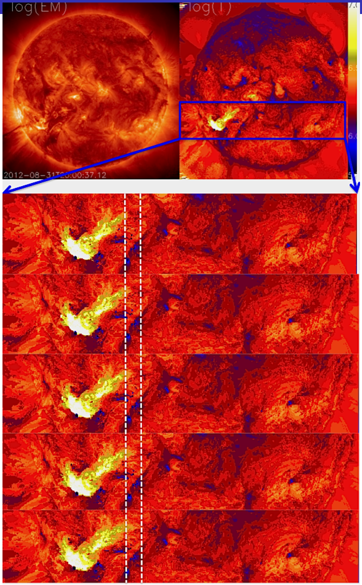

# Original Temperature Maps of 3 cases:

(1) Flare event: GOES-class C8 at 20:00 UT in NOAA active region 1562.

(2) No flare: same active region at 15:00 UT.

(3) Quiet Sun: SE region at 20:00 UT. (snapshots every 5 minutes)

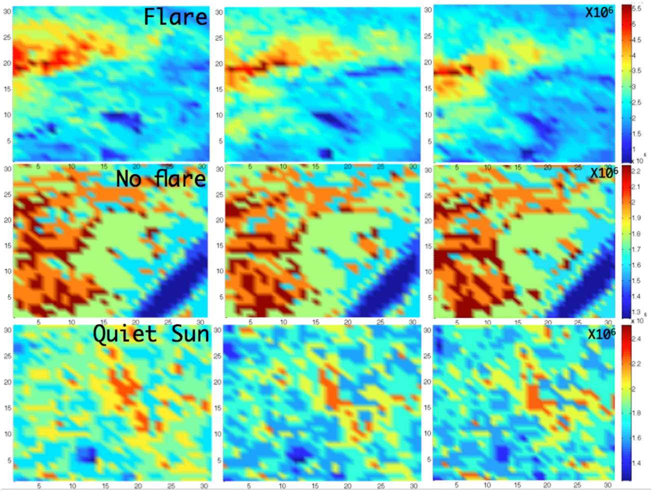

# Temperature Maps Analysis:

## T-Maps processing using POD

The POD methods, based on the Singular Value Decomposition (SVD), build a new base in which the data is represented in an optimal way.

This method is used to extract dominant features and coherent structures by identifying and organizing the dimensions in which the data exhibits more variation.

Once identified where there is more variation, it is possible to find the best approximation of the original data using fewer dimensions (truncation to a smaller range of the size of the original matrix).

- Topos-Cronos
- GLRAM

# T-Maps Analysis: math basis

Singular Value Decomposition (SVD) is based on the factorization of matrix A as follows:

$$A = U \Sigma V^T,$$

Seen as a sum of tensor product:

$$A = \sum_{ij} A_{ij} = \sum_{k=1}^{N_{DVS}} \sigma^k u^k(x_i) v^k(y_j)$$

where: $N_{DVS} = min\{N_x, N_y\}$.
Eckart-Young Theorem states that $A^{(r)}$ is the optimum aproximation to the matrix A.

$$\parallel A - A^{(r)} \parallel^2 = min\{\parallel A - B \parallel^2 |rank(B) = r\}$$

$$A^{(r)} = \sum_{k=1}^{r} \sigma^k u^k(x_j) v^k(y_j)$$

- (Independet) Spatial and Temporal representation of the original data matrix.
- Using the coordinate transformation: $r_i \longleftarrow (x_i, y_j)$ to $T_i(x, y)|_{t_j}$ we get $T(r_i, t_j)$, with dimension: $N_x N_y \times N_t$.
- The rank $r$ tensor product decomposition of $T$ is given by:

$$T^r(r_i, t_j) = \sum_{k=1}^{r} \sigma^k u^k(r_i) v^k(t_j),$$

where $1 \leq r \leq N^*$ y $N^* = \min[N_x N_y, N_t]$.

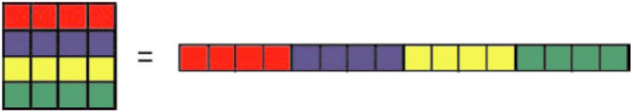

$(x_i, y_j) \longrightarrow r_i$

# Topos Chronos-Solar Flare

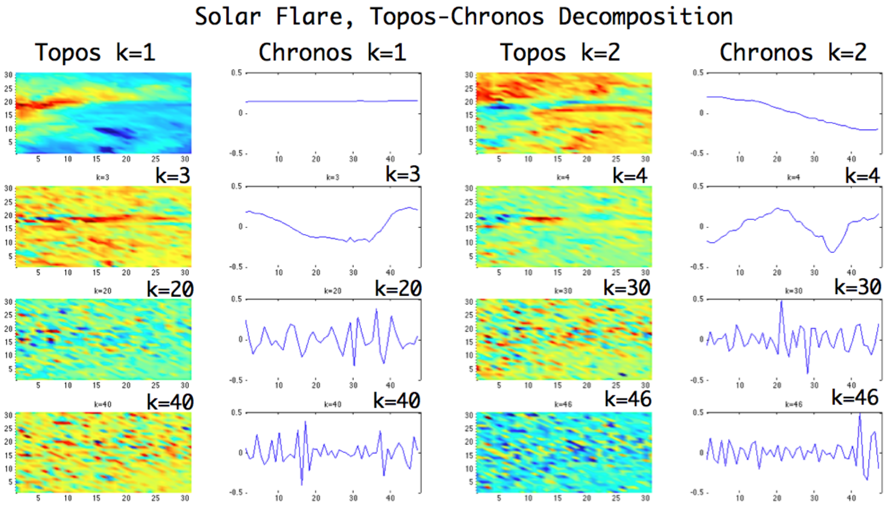

# Topos Chronos-No Flare, same AR

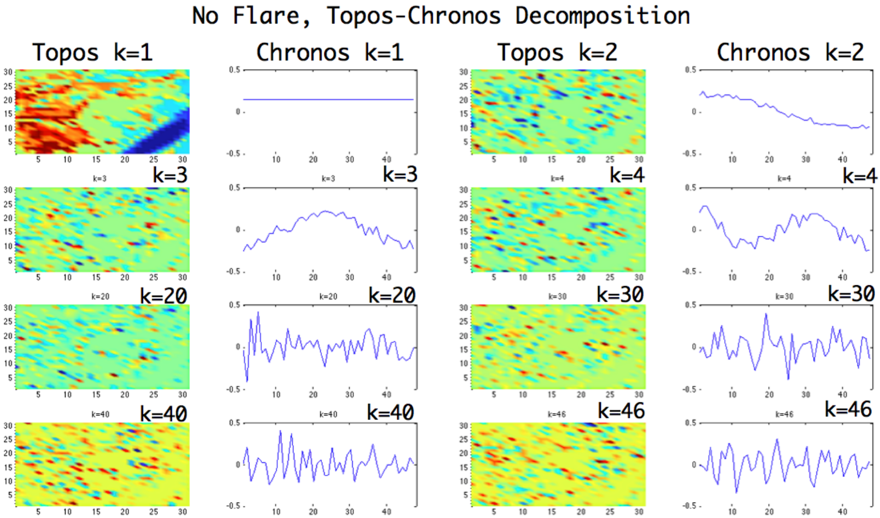

# Topos Chronos-Quiet Sun

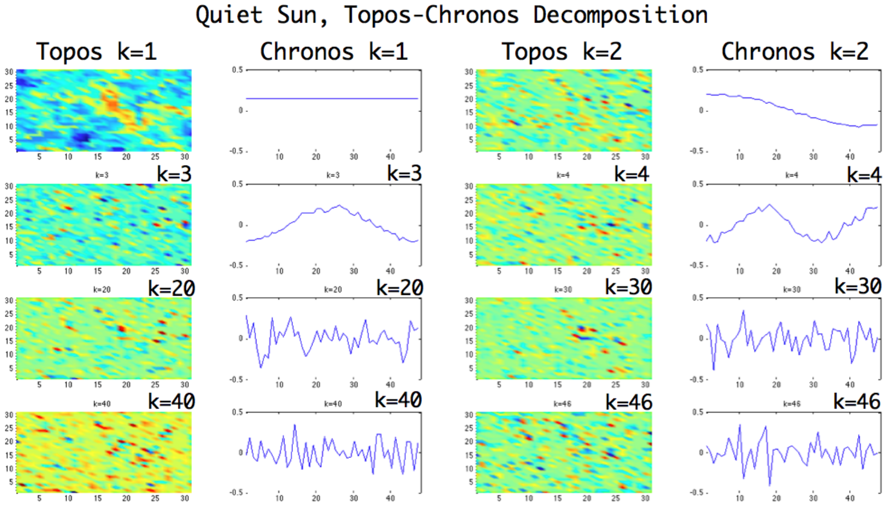

## Multi-scale Analysis

-Dominant mode: k=1.

- Low $k$ exhibit low frequency variation and high $k$ exhibit high frequency activity.

- Spatial scales diminish with $k$ - granular type.

- Correlation between spatial and temporal scales as a function of rank should exist.

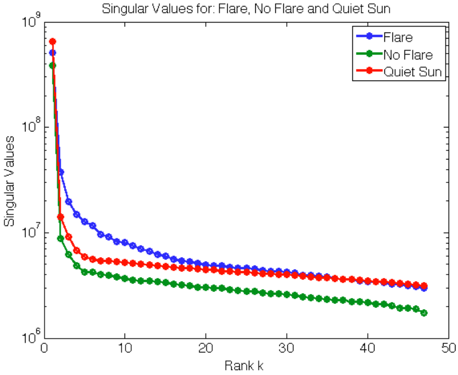

# Spatio-Temporal Correlation

Topos: Fourier Transform in $x_i$ and $y_j$ (folding unidimensional vector $r_i$) of $u_k \rightarrow \hat{u}_k(\kappa_{xi}, \kappa_{yj})$.

The characteristic length scale of rank-k is defined by: $\lambda(k) = 1/\langle\kappa\rangle$, where $\langle\kappa\rangle$ is defined as follows:

$$\langle\kappa\rangle = \frac{\Sigma_{i,j}|\hat{u}_k(\kappa_{xi}, \kappa_{yj})|^2(\kappa_{xi}^2 + \kappa_{yj}^2)^{1/2}}{\Sigma_{i,j}|\hat{u}_k(\kappa_{xi}, \kappa_{yj})|^2}$$

Chronos Similarly with temporal scale $\tau$. FFT of $v_k(t_m) \rightarrow \hat{v}_k(f_m)$ defines $\tau(k) = 1/\langle f\rangle$ with:

$$\langle f\rangle = \frac{\Sigma_m|\hat{v}_k(f_m)|^2 f_m}{\Sigma_m|\hat{v}_k(f_m)|^2}$$

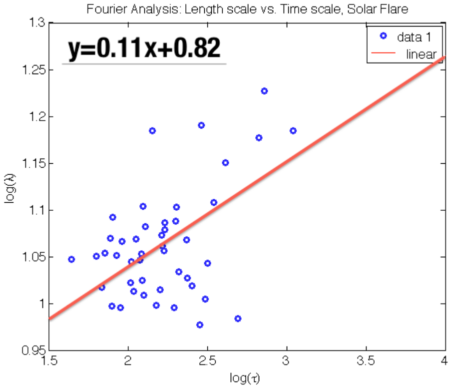


## Solar Flare case

Cascade process associated with non-diffusive transport: $\lambda \sim \tau^{\chi}$ with $\chi \neq 1/2$.

For the rest of the cases, no tendency was found.

No Flare

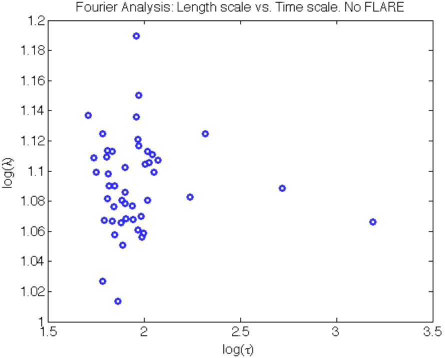


Quiet Sun

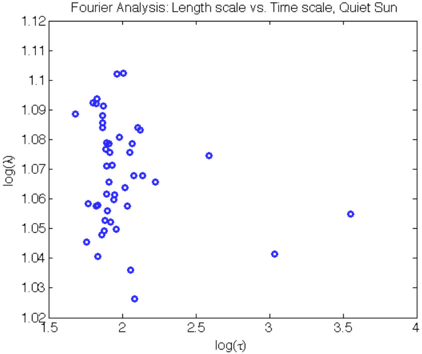

# Statistical Analysis - PDF

## Energy Contribution of the rank-k reconstruction

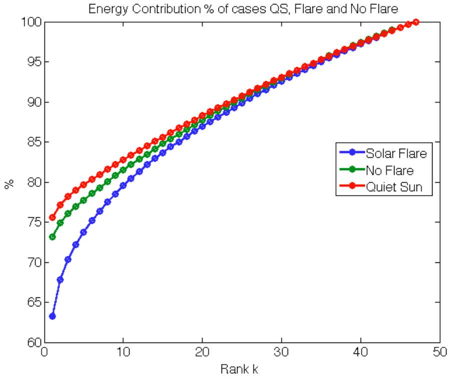


Energy content: $E = \sum_{k=1}^{N^*} \sigma_k^2$

$\sigma_k^2$ gives the energy contribution of the $k$th-mode, and since $\sigma_k \geq \sigma_{k+1}$, the POD can be seen as a decomposition of the data in terms of the energy content.(Futatani 2009)

Reconstruction error: Mean of rescaled PDFs given by:

$$RT = T_{or} - T^k$$

where $RT$ measures the fluctuations.
PDFs
PDFs calculated in space 31×31 divided in boxes, rescaled with $\sigma$, averaged over time and normalized.

Stretched Exponential fit:

$$F(\mu, \beta) \propto exp[-\beta \mid x \mid^{\mu}]$$

# Normalized mean of rescaled PDF for % energy

~75% ~85% ~90%

Flare

No flare

QS

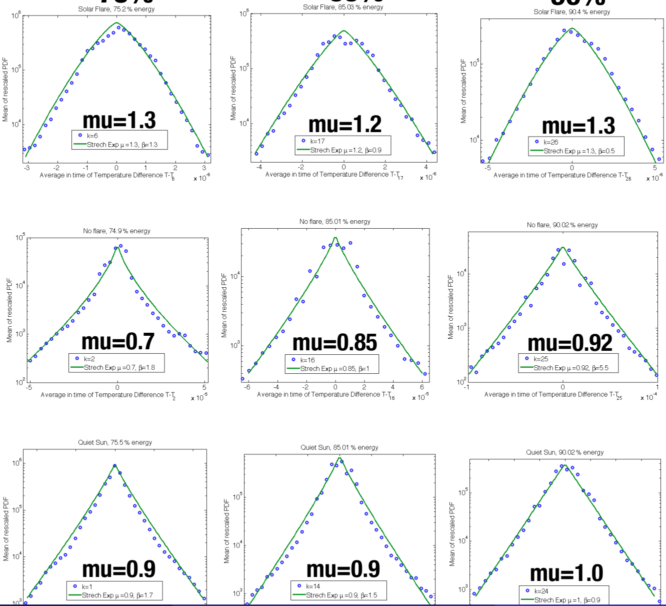

# Normalized PDF of temperature fluctuations

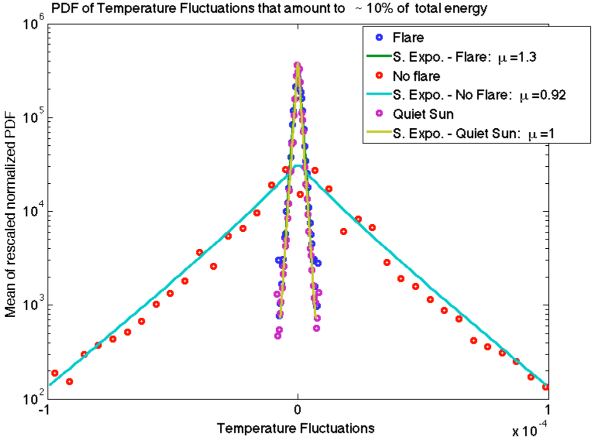


-For Gaussian PDF the process is diffusive and non-chaotic.

-Intermittency arise in turbulent processes and these produce long tails in pdf (Futatani 2009). Without sources thre is no intermittency.

Results:

-Intermittency observed a few hours before the solar flare takes place.

-In QS region no intermittency is registered.

-After Solar Flare event there is no intermittency and pdfs tend to the Gaussian.

- Matrix approximation at any rank is again given by the SVD, except that in this method matrices $U$ and $V$ are independent of time, temporal information stored in the singular values matrix ($M_j$).
- $\min \sum_{i=1}^{n} \| T_i - LM_iR^T \|_F^2$ .

Original

GLRAM

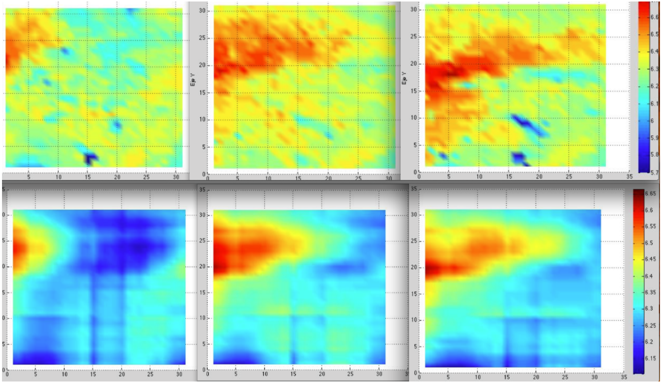

# GLRAM

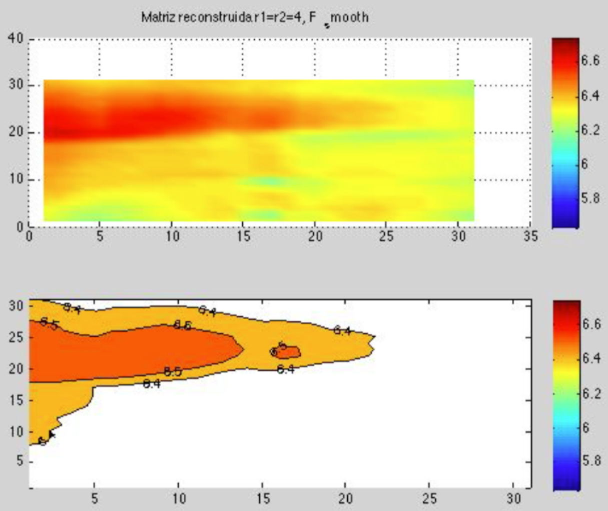

Matriz reconstruida r1=r2=4, F smooth
40
30
20
10
0
0
5
10
15
20
25
30
35
6.6
6.4
6.2
6
5.8
30
25
20
15
10
5
5
10
15
20
25
30
6.4
6.5
6.4
6.5
6.4
6.5
6.5
6.4
6.4
6.6
6.4
6.2
6
5.8

## Area Method

One way to measure the diffusion is by calculating the area $A$ variation between two fronts of the thermal pulse, $T_1$ and $T_2$, where $T_1 < T_2$. Thus we can see directly the relation: $A \sim \sigma^2 \sim t^\gamma$.

### Normal Diffusion

From the Gaussian distribution of temperature:

$$T_i(r_i, t) = \frac{1}{\sqrt{4\pi t}} e^{-\frac{|r_i|^2}{4t}}$$

it follows that

$$\triangle A = 4\pi t \left[\log\left(\frac{T_2}{T_1}\right)\right] \sim t \quad ,$$

### Anomalous Diffusion

The solution of the fractional diffusion equation has an algebraic decay (like the Lévy function).

The area between two temperatures comes from the Green function of the fractional diffusion equation in which: $\langle r_i \rangle \propto [G(\eta_i)] t^{\gamma/2}$, therefore:

$$\Delta A \propto \pi [G(\eta_2)^2 - G(\eta_1)^2] t^\gamma \sim t^\gamma \quad ,$$

# Results

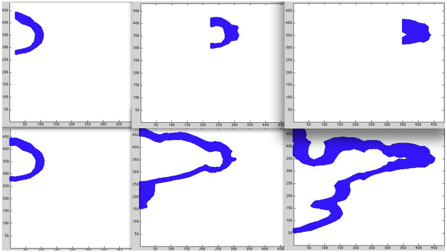

## Conclusions

- POD methods provide an excelent tool for analyzing observations and provide information on the underlying physical processes.
- **Topos-Chronos**: Intermittency is present in active regions before appearance of solar flare but not in quiet regions.
- **Transport** The multi-scale analysis shows a "slow" cascade energy process which is non-diffusive with $\lambda \propto \tau^{0.19}$.
- **GLRAM**: The area (point count) at each time between two contours goes like: $A_{21} \propto t^{0.77}$, i.e. $\gamma = 0.77$, which implies that the type of transport is *subdiffusive*.

## Comments

- Temperature maps have low spacial (400px) and temperature value resolution (27 values), therefore is difficult to distinguish the propagation of a thermal pulse.

- More events have to be analyzed the work is still in process.

# References


Wiegelmann et al. *Similarities and differences between coronal holes and quiet sun: Are loops statistics the Key?*, *Solar Physics* **225** 227-247 (2004).

S. Futatani, S. Benkadda, D. del-Castillo-Negrete. *Spatiotemporal multiscaling analysis of impurity transport in plasma turbulence using proper orthogonal decomposition*, Physics of Plasmas, **16** 042506, (2009).

M.J. Aschwanden et al. *Automated Temperature Emission Measure Analysis of Coronal Loops and Active Regions Observed with SDO/AIA Solar Physics* **283** 5-30 (2011)

D. del-Castillo-Negrete, S.P. Hirshman, D.A. Spong, D.A. D'Azevedo, *Compression of magnetohydrodynamic simulation data using singular value decomposition*. Journal Of Computational Physics, **222**, 265 (2007).

J. Ye, Generalized low rank approximations of matrices, Mach. Learn. **61**, 167-196, 2005.

# Solar Flare case: Total Heat Flux of thermal pulse

**For the characterization of the transport of heat of the thermal pulse we considered that:**

1. Heat Flux only along X axis.
2. Heat Flux of thermal pulse has two components, one due to convection and a the other diffusion (electrons).
3. Large field limit ($\omega_{c\alpha}\tau_\alpha \gg 1$, $\alpha = i, e$).
4. Internal Energy: $u = \frac{3}{2} n k_B T$ (monoatomic plasma), no work done ($W = 0$ y $dU = Q$).
5. Constant density in time and uniform in space.
6. Control Volume: $\Delta V = \Delta x \Delta y \Delta z = \dfrac{L_x \times L_y \times h}{N_{Xpix} \times N_{Ypix}} = \dfrac{L^2 h}{N^2}$ where $h$ is the width of the TR and $\lambda = (6\mathrm{arcsec} \times 7.15 \times 10^5 \mathrm{m})$ is the conversion factor from pixels to meters.

# Heat Flux Diagram- Control Volume.

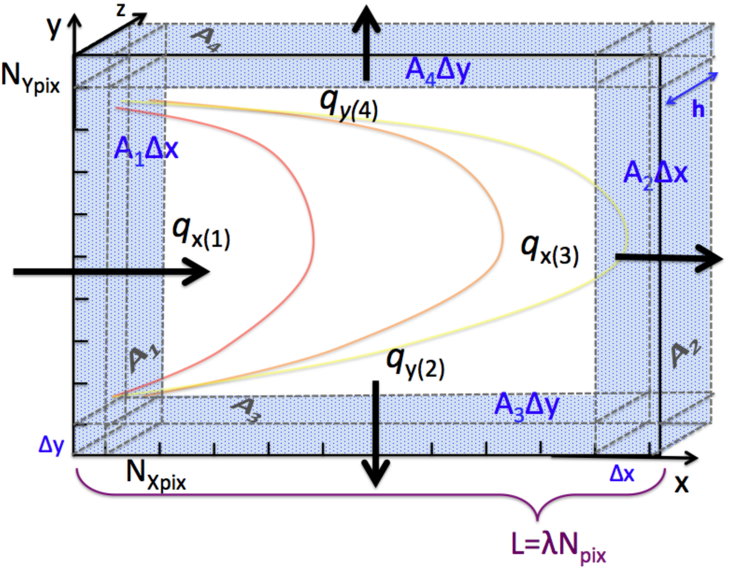

# Total Heat Flux of the thermal pulse

The Total Heat Flux of the thermal pulse in the control volumne is given by:

$$\frac{3nk_B}{2}\frac{d}{dt}\iiint_V TdV = \frac{3nk_B}{2}\frac{d}{dt}\left[\sum_{i=1}^{N_xN_y}\sum_{k=1}^{N^*}\sigma^k u^k(r_i)v^k(t_j)\Delta V\right] = \oiint_A \vec{q}_{Tot}\cdot d\vec{A} \qquad , \qquad (1)$$

where $1 \leq r \leq N^*$ y $N^* = \min[N_xN_y, N_t]$.

Using only the first mode (r=1), the heat flux entering the is:

$$\frac{q_1}{k_B}|_{t_j} = \frac{3}{2}\frac{nL}{N^2}\sigma^1\left[\sum_{i=1}^{N_xN_y} u^1(r_i)\right]\frac{dv^1}{dt}|_{t_j} \quad . \qquad (2)$$

averaged over time gives:

$$\frac{\langle q_1\rangle_t}{k_B} = 1.618\times 10^{26}\mathrm{Km}^{-2}\mathrm{s}^{-1}$$

Using: $n = 10^{15}\ \mathrm{m}^{-3}$, T=2.5 to 3.5 MK and convective velocity determined with GLRAM, the mean of the convective flux is given by:

$$\frac{\mathrm{q}_u}{k_B} = nT_eu_x = 1.85\times 10^{26}\mathrm{K/m}^2 s$$

This means that convection governs the transport of heat of the thermal pulse.